

See discussions, stats, and author profiles for this publication at: <https://www.researchgate.net/publication/260272035>

Synthesis and Catalytic Reactions of Nanoparticles formed by Electrospray Ionization of Coinage Metals

ARTICLE *in* ANGEWANDTE CHEMIE INTERNATIONAL EDITION · MARCH 2014

Impact Factor: 11.26 · DOI: 10.1002/anie.201309193 · Source: PubMed

CITATIONS

14

READS

72

4 AUTHORS, INCLUDING:



Anyin Li

Purdue University

15 PUBLICATIONS 112 CITATIONS

SEE PROFILE

Synthesis and Catalytic Reactions of Nanoparticles formed by Electrospray Ionization of Coinage Metals**

Anyin Li, Qingjie Luo, So-Jung Park, and R. Graham Cooks*

Abstract: Noble metals can be ionized by electrochemical corrosion and transported by electrospray ionization. Mass spectrometry (MS) showed solvated metal ions as the main ionic constituent of the sprayed droplets. Collection of the electrospray plume on a surface yielded noble metal nanoparticles (NPs) under ambient conditions. The NPs were characterized by several techniques. Under typical conditions, capped-nanoparticle sizes averaged 2.2 nm for gold and 6.5 nm for silver. The gold nanoparticles showed high catalytic activity in the reduction of *p*-nitrophenol by NaBH_4 . Efficient catalysis was also observed by simply directing the spray of solvated Au^+ onto the surface of an aqueous *p*-nitrophenol/ NaBH_4 mixture. Organometallic ions were generated by spiking ligands into the spray solvent: for example, Cu^I bipyridine cations dominated the spray during Cu electrocorrosion in acetonitrile containing bipyridine. This organometallic reagent was shown to be effective in the radical polymerization of styrene.

The coinage metals are of widespread interest for their optical, physical, and chemical properties. Despite their stability, versatile chemical reactivity has been discovered for these elements in their oxidized states^[1] as well as in the nanoscale form.^[2] Current methods of metal nanoparticle (NP) preparation involve dissolution by oxidation of the metal using strong acidic reagents like aqua regia, followed by reduction and, sometimes, by coordination (“capping”).^[3]

Electrolysis is also an effective way to release metals into solution, and it has been used to generate NPs.^[4,5]

Electrochemical reactions occur during electrospray ionization (ESI) mass spectrometry.^[6] When carried out in typical protic solvents, electrolysis of water is usually the dominant process but its products (protons and O_2) have little impact on the resulting mass spectra of most analytes. Greater electrochemical influence is observed when ESI is performed at low flow rates (nanoESI) and/or at high-current^[7] conditions.^[8] Unconventional (nonpolar, anhydrous, aprotic, etc.) solvents have seen little use in ESI MS,^[9] while they are common in synthetic chemistry.^[10]

Electrospray deposition utilizes dispersed plumes of charged droplets as carriers for dissolved reagents to fabricate structures like thin films.^[11] A parallel mass-spectrometry experiment collects mass-selected ions at surfaces, that is, performs ion soft-landing.^[12] In this work we combine electrocorrosion in a nonprotic solvent with transport of the solvated metal ions by the electrospray plume to synthesize metal nanoparticles in an ambient environment.

To obtain the coinage-metal nanoelectrospray ion source, a wire-in-a-capillary nanoelectrospray emitter^[8a] was fitted with a metallic silver anode. The mass spectrum showed no metal containing ions when spraying $\text{MeOH}/\text{H}_2\text{O}$ solvent. However, with anhydrous acetonitrile, electrocorrosion of silver occurred and silver-containing ions (Figure 1) appeared

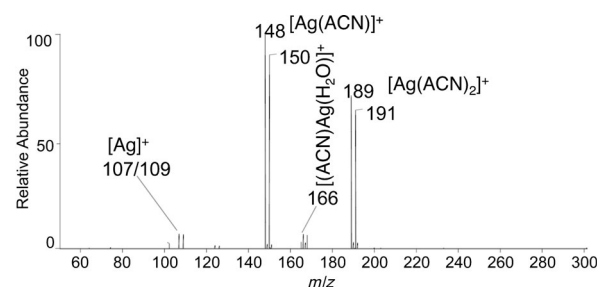


Figure 1. Mass spectrum recorded 1 min after starting electrocorrosion/nanoelectrospray of metallic silver in acetonitrile (ACN) in a nano-ESI ion source. Silver-containing ions are labeled.

in the spectrum within ten seconds, which is probably the time needed to consume the trace amount of adventitious water taken up when handling solvents under ambient conditions. Data similar to those shown in Figure 1 were recorded using gold and copper electrodes (see Figure S1 in the Supporting Information). Whereas electrospraying salt solutions generates anion/cation cluster ions,^[13] this experiment yielded simple solvated metal ions only. The number and concen-

[*] A. Li,^[‡] Prof. R. G. Cooks

Department of Chemistry, Purdue University
West Lafayette, IN 47907 (USA)
E-mail: cooks@purdue.edu

Q. Luo,^[‡] Prof. S. Park

Department of Chemistry, University of Pennsylvania (USA)
Prof. S. Park
Department of Chemistry and Nano Science
Ewha Womans University (Korea)

[‡] These authors contributed equally to this work.

[**] We acknowledge financial support from the Separations and Analysis Program, Office of Basic Energy Sciences, US Department of Energy, DE-FG02-06ER15807. Generous help and insightful discussions with Yang Gao (Purdue University), Xiaobo Zhu (Temple University), Na Zhang (University of Pennsylvania), Shampa Samanta (University of Pennsylvania), Zhaoxia Qian (University of Pennsylvania), and Christopher J. Gilpin (Purdue Life Science Microscope Facility) are acknowledged. We acknowledge the use of Purdue's Biological Electron Microscopy Facility, a facility of the NIH funded Indiana Clinical & Translational Science Institute.

Supporting information for this article is available on the WWW under <http://dx.doi.org/10.1002/anie.201309193>.

tration of (solvated) metal ions generated in the electrospray plume can be estimated from the measured ion current and the solution flow rate. Typical ion fluxes were 6.2×10^{10} per second (10 nA) and solution flow rates were 10 nL min^{-1} , yielding an estimated concentration of metal containing ions in the spray plume of $10 \text{ }\mu\text{M}$ (ca. 1.5 ppm).

This ion source produces metal ions in charged droplets virtually free of counterions (Figure S2). Direct deposition of the electrospray plume allows neutralization, solvent evaporation, and aggregation of the metal at the grounded cathode surface, although details of the mechanism have not been elucidated. Deposition of solvated Au^+ droplets onto a stainless-steel plate yielded colored micro-objects observable by the naked eye. The generation of nanosized metal particles on the surface was verified by placing a transmission electron microscope (TEM) grid on the surface and repeating the collection. The TEM micrograph showed nanosized metal particles (Figure 2a). The AuNP composition was confirmed

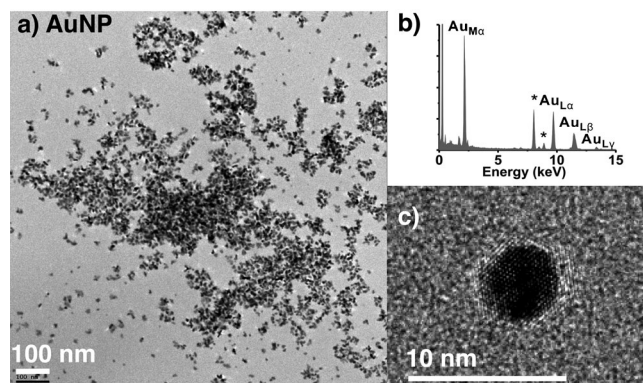


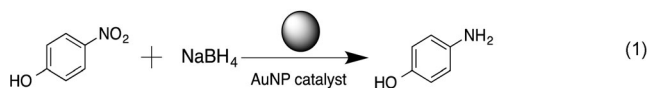
Figure 2. a) Au nanoparticles synthesized by electrocorrosion/nanoESI of gold and deposition of the solvated gold ions onto a TEM grid. b) EDX spectrum taken from the central area of (a) with a Tecnai G20 electron microscope (peaks labeled as * are copper from the TEM grid). c) High-resolution TEM image of the same sample recorded using a Titan Krios electron microscope showing lattice fringes of the AuNP.

by elemental analysis using EDX (Figure 2b and Figure S3, S4). At higher spatial resolution (Figure 2c) the TEM experiment showed the expected lattice fringes and diffraction patterns characteristic of crystalline gold (Figure S5, S6). This established that the particles are crystalline and metallic as opposed to metal oxide aggregates. This was further verified by the metal signals seen in laser desorption MS (Figures S7–S9) and by the catalytic activity discussed below. The particles are clearly polydispersed in size (Figure S10).

Metal-ESI-based nanoparticle synthesis also occurred when the spray was directed onto the surface of a solution. Solvents examined were water and toluene, with both of which ACN is miscible, making the ion source applicable to NP preparation in both phases. Data are given in the Supporting Information (Table S1). Standard methods of solution-phase nanoparticle synthesis using redox chemistry rely on capping reagents to control NP size and avoid

aggregation.^[14] As summarized in Table S1, the addition of capping ligands to the receiving solution in the spray-deposition experiments significantly improved the size distribution of the observed nanoparticles. The narrower size distributions of gold and silver nanoparticles are evident from Figure S11.

The catalytic activity of nanoparticles is frequently evaluated using the reduction of 4-nitrophenol by NaBH_4 in aqueous solution [Eq. (1)], with UV/Vis absorption being



used to monitor the progress of the reaction. This experiment was done under various conditions (Figure 3) with AuNPs prepared offline. Analysis of the reaction kinetics gave a rate constant k of 0.0279 s^{-1} , which is comparable to the highest literature value (0.0472 s^{-1} ^[15]) and is one or two orders of magnitude higher than that for other commonly synthesized AuNPs (Table S2).

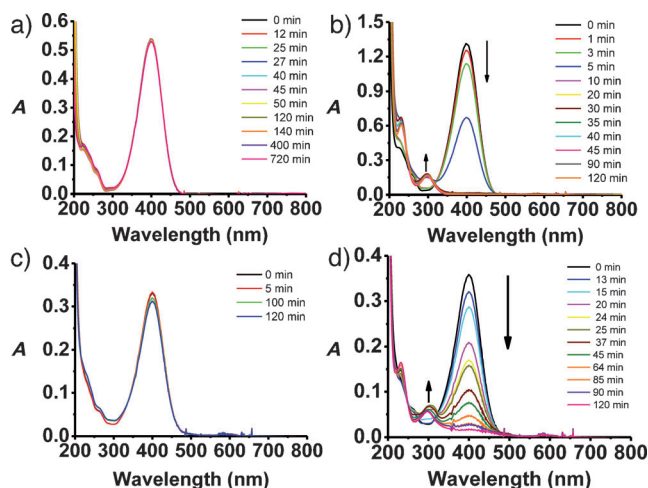


Figure 3. Nanoparticles prepared offline or online catalyze reaction (1). Overlays of selected UV/Vis spectra of the reaction mixture monitored every 30 s (only larger intervals are shown) show the major peak at 400 nm ($n \rightarrow \pi^*$ transition of the *p*-nitrophenol anion) decreasing in (b) and (d) in the course of reduction. a) Without AuNPs, the reaction did not occur at all within 12 h. b) Addition of offline prepared electrosprayed AuNPs led to complete reaction within 30 min. c) A control experiment performed by spraying a protic solvent into the reaction mixture demonstrates that the reaction is not influenced by cathodic currents. d) Online addition of charged droplets containing Au^+ ions instead of AuNPs, achieved by spraying ions (10 nA) onto the surface of the reaction mixture, shows that extremely small amounts of gold catalyze the reduction.

As an alternative to separating the synthesis of the nanoparticles from their addition to a reaction mixture, solvated Au^+ ions were sprayed directly onto the surface of the reaction solution. The reaction mixture was electrically grounded, the spray rate was 10 nA, and the UV/Vis spectrum was monitored continuously. The amount of Au involved was very small (ca. $1.2 \times 10^{-8} \text{ mg mL}^{-1} \text{ s}^{-1}$) compared to that used

in the offline AuNP experiments (2.6×10^{-4} mg mL⁻¹). Figure 3d shows that reaction product is discernible after 20 min; at this time 7.2×10^{-6} mg mL⁻¹ of Au had been introduced. This mode of catalysis is highly efficient (see Section 3 in the Supporting Information) and also “one-pot” by eliminating offline nanoparticle synthesis. It was also found that in the presence of cetyltrimethylammonium bromide (CTAB) as a capping ligand the apparent reaction rate constant rose to 8×10^{-6} s⁻², which is significantly higher than that without capping ligand (8×10^{-7} s⁻²; Table S2). The higher catalytic activity in the presence of capping ligands is attributed to their ability to reduce the aggregation of smaller NPs and clusters, which have higher surface areas and catalytic efficiencies.^[16] Directly spraying the metal ions into the reaction mixture is effective in generating product, presumably through in situ formation of NP catalysts.

Cu^I and Au^I complexes are highly reactive species that serve as catalysts for many reactions,^[17] and the coinage-metal nanoelectrospray ion source is an effective way to generate organometallic ions through addition of ligands such as phen, bpy, and PPh₃ in low concentrations (ca. 1 ppm) to the acetonitrile spray solvent. The ligands do not seem to influence the overall anode electrolysis but they readily bind to the metal cations (or replace weakly bound acetonitrile) to form the corresponding organometallic ions.

Like harvesting metals in the form of nanoparticles, it might be similarly useful to collect organometallic compounds by ion deposition. [(bpy)₂Cu]⁺ ions are catalysts in solution-phase atom transfer radical polymerization^[18] and were chosen to test for a similar capability of the material derived under the mild conditions of electrospray ionization. Droplets containing [(bpy)₂Cu]⁺ ions were collected under ambient conditions in 10 mM HCl in ACN. After collection of 4.3 μg (estimated from the current) the solution was transferred to a Schlenk flask and dried using a N₂ flow. Then styrene (8.73 mmol) and azobis(isobutyronitrile) (AIBN; 0.039 mmol) were added. After overnight reaction, the polymer obtained was better monodispersed than that from control experiments (Figure S14), a demonstration of catalytic activity.

The synthesis of NPs without use of explicit redox reagents has been described herein. The resulting NPs have been characterized and initial applications in catalysis detailed. The electrocorrosion process is “top-down”, but mechanistically the aggregation of material from isolated solvated ions makes this an example of “bottom-up” NP synthesis.^[19] Much remains to be learned regarding the mechanism of NP synthesis by nanoelectrospray. The counter-ion-free metal-ion source should find application in the synthesis of a wide range of nanomaterials. The demonstrated ability to focus and direct ions in air^[20] should make writing on surfaces possible.

Experimental Section

Nanoparticle synthesis

A high-voltage supply (Bertan 205B-05R) was connected through a 120 MΩ resistor to the electrospray electrodes. The grounded

cathode was connected to a Keithley 428 current amplifier used with *I/V* conversion ranging from 10⁷ to 10⁹. The output of the amplifier was monitored by a dual-channel oscilloscope (Fluke 199C).

Dodecanethiol, CTAB, NaBH₄, sodium citrate, and mercaptopoly-(ethylene glycol) monomethyl ether (PEG-SH, Mn 2000) were purchased from Sigma Aldrich, *p*-nitrophenol (reagent grade) from Fluka, and acetonitrile (99.9%, Extra Dry, AcroSeal, M-cap) from Acros Organics, and used as received. Deionized water (Millipore Milli-Q grade) with a resistivity higher than 17.9 MΩ was used. A microelectrode holder with silver wire from Warner Instruments was used as the holder for the electrospray emitter. Gold wire (0.1 mm, 99.998%) was purchased from Alfa Aesar. Copper wire was stripped from a 22 gauge coaxial cable (plenum style RG 62). The metal wires replaced the silver wire in the microelectrode holder as needed. The electrospray emitters were prepared from borosilicate glass tubing (Sutter Instruments) using a micropipette puller (p-97, Sutter Instruments). Grounded stainless-steel plates with TEM grids on top were used as the dry collecting surface. A grounded copper tape (Mouser electronics) was formed into a concave shape to hold solution reagents for the wet nanoparticle synthesis. The quantities of reagents used for the various NP synthesis experiments are recorded in Table S1. Grids (CF200-Cu, Electron Microscopy Science) were used to hold prepared nanoparticle samples that were imaged using a Tecnai T12 transmission electron microscope. Size analysis from the TEM images used the ImageJ program. EDX analysis was performed in a FEI Tecnai G20 electron microscope. High-resolution imaging was performed in a Titan Krios electron microscope. LDI-MS was performed in a Voyager-DE Pro mass spectrometer.

Catalytic reduction of *p*-nitrophenol

The reactions were carried out inside a quartz cuvette of 1 cm path length. The reaction mixture contained water, *p*-nitrophenol, and NaBH₄. The catalyst was added in the form of an AuNP solution prepared offline or in the form of Au⁺ containing droplets in the online catalyst synthesis. The quantities of reagents used for each trial are shown in Table S2. Before adding the catalyst, UV/Vis absorption of the reaction mixture was monitored for 2 min to make sure that there was no AuNP contamination from previous experiments. The nanoparticle catalyst was added and UV spectra were recorded at 30 s intervals for 2 h. The progress of the reaction was monitored in situ using the UV/Vis data (Agilent 8453) while the reaction temperature was held constant at 25 °C. When Au⁺ containing droplets were sprayed into the cuvette, a larger volume of reaction solution was used so that the top surface was about 5 mm from the Au⁺ emitter.

Catalytic polymerization

Styrene (99%, Sigma) was passed through a short Al₂O₃ column prior to use to remove inhibitor. AIBN (Sigma) was used as received. The procedure for the homogeneous reverse atom transfer radical polymerization of styrene was described previously.^[17b] In a typical experiment, 1 mL of styrene (0.909 g, 8.73 mmol), AIBN (6.4 mg, 0.039 mmol), were mixed in a Schlenk flask, without (control experiment) or with (actual run) the collected organometallic copper compound, estimated (by integrating landing current) to be about 10.4 nmol [(bpy)₂Cu]⁺ (equivalent to 4.3 μg [(bpy)₂Cu]Cl). Three “freeze–pump–thaw” cycles were performed to remove oxygen from the solution. The flask was immersed into an oil bath at (110 ± 2) °C and allowed to react for 12 h. Then the flask was removed from the oil bath and cooled to room temperature. Polymerization was quenched by opening the flask to room air. Afterwards, the reaction mixture was dissolved in 0.5 mL THF and washed with excess methanol. The polymeric precipitate was collected by centrifugation at 8000 rpm for 10 min and the supernatant removed. The polymer was redissolved in THF to make a solution with a concentration of about 1 mg mL⁻¹ for further analysis.

In the control experiment, a Schlenk flask of 30 μL (ACN with 10 mM HCl) was dried by passing dry nitrogen until the liquid had

evaporated and then 1 mL of styrene (8.73 mmol) and of AIBN (0.039 mmol) were added. The rest of the procedure was the same as above.

Gel permeation chromatography (GPC) analysis of the polymer samples was done using high-performance liquid chromatography (PerkinElmer Series 10; LC-100 column oven (40 °C), Nelson Analytical 900 Series integration data station, PerkinElmer 785 UV/Vis detector (254 nm), Varian star 4090 refractive index detector, and three AM gel columns (500 Å, 5 µm; 1000 Å, 5 µm; and 104 Å, 5 µm)). THF (Fisher, HPLC grade) was used as eluent at a flow rate of 1 mL min⁻¹. The number-average (M_n) and weight-average (M_w) molecular weights of the PS samples were determined with polystyrene standards purchased from American Polymer Standards.

Received: October 21, 2013

Revised: December 12, 2013

Published online: February 19, 2014

Keywords: electrocorrosion · gold catalysis · heterogeneous catalysis · nanoparticles · polymerization

- [1] A. Corma, A. Leyva-Perez, M. J. Sabater, *Chem. Rev.* **2011**, *111*, 1657–1712.
- [2] a) M. Haruta, *Nature* **2005**, *437*, 1098–1099; b) A. S. K. Hashmi, G. J. Hutchings, *Angew. Chem.* **2006**, *118*, 8064–8105; *Angew. Chem. Int. Ed.* **2006**, *45*, 7896–7936; c) S. Eustis, M. A. El-Sayed, *Chem. Soc. Rev.* **2006**, *35*, 209–217.
- [3] P. I. Varghese, T. Pradeep, A. Ashokreddy, *A Textbook of Nanoscience and Nanotechnology*, Tata McGraw Hill Education, New Delhi, **2012**.
- [4] a) N. Vilar-Vidal, M. C. Blanco, M. A. Lopez-Quintela, J. Rivas, C. Serra, *J. Phys. Chem. C* **2010**, *114*, 15924–15930; b) Y. C. Liu, L. H. Lin, W. H. Chiu, *J. Phys. Chem. B* **2004**, *108*, 19237–19240.
- [5] A. I. Yanson, P. Rodriguez, N. Garcia-Araez, R. V. Mom, F. D. Tichelaar, M. T. M. Koper, *Angew. Chem.* **2011**, *123*, 6470–6474; *Angew. Chem. Int. Ed.* **2011**, *50*, 6346–6350.
- [6] J. F. de La Mora, G. J. Van Berkel, C. G. Enke, R. B. Cole, M. Martinez-Sanchez, J. B. Fenn, *J. Mass Spectrom.* **2000**, *35*, 939–952.
- [7] G. J. Van Berkel, V. Kertesz, *Anal. Chem.* **2007**, *79*, 5510–5520.
- [8] a) G. J. Van Berkel, K. G. Asano, P. D. Schnier, *J. Am. Soc. Mass Spectrom.* **2001**, *12*, 853–862; b) X. M. Xu, S. P. Nolan, R. B. Cole, *Anal. Chem.* **1994**, *66*, 119–125; c) X. M. Xu, W. Z. Lu, R. B. Cole, *Anal. Chem.* **1996**, *68*, 4244–4253.
- [9] A. Li, H. Wang, Z. Ouyang, R. G. Cooks, *Chem. Commun.* **2011**, *47*, 2811–2813.
- [10] C. Reichardt, T. Welton, *Solvents and Solvent Effects in Organic Chemistry*, 4th ed., Wiley-VCH, Weinheim, **2011**.
- [11] a) V. N. Morozov, T. Y. Morozova, *Anal. Chem.* **1999**, *71*, 1415–1420; b) A. Jaworek, *J. Mater. Sci.* **2007**, *42*, 266–297; c) A. K. Badu-Tawiah, A. Li, F. P. M. Jjunju, R. G. Cooks, *Angew. Chem.* **2012**, *124*, 9551–9555.
- [12] a) V. Franchetti, B. H. Solka, W. E. Baitinger, J. W. Amy, R. G. Cooks, *Int. J. Mass Spectrom. Ion Processes* **1977**, *23*, 29–35; b) J. L. Benesch, B. T. Ruotolo, D. A. Simmons, N. P. Barrera, N. Morgner, L. Wang, H. R. Saibil, C. V. Robinson, *J. Struct. Biol.* **2010**, *172*, 161–168; c) S. Rauschenbach, F. L. Stadler, E. Lunedei, N. Malinowski, S. Koltsov, G. Costantini, K. Kern, *Small* **2006**, *2*, 540–547; d) G. E. Johnson, T. Priest, J. Laskin, *J. Phys. Chem. C* **2012**, *116*, 24977–24986.
- [13] G. D. Wang, R. B. Cole, *Anal. Chim. Acta* **2000**, *406*, 53–65.
- [14] a) R. Sardar, A. M. Funston, P. Mulvaney, R. W. Murray, *Langmuir* **2009**, *25*, 13840–13851; b) M. C. Daniel, D. Astruc, *Chem. Rev.* **2004**, *104*, 293–346; c) V. Dixit, J. Van den Bossche, D. M. Sherman, D. H. Thompson, R. P. Andres, *Bioconjugate Chem.* **2006**, *17*, 603–609.
- [15] J. Zeng, Q. Zhang, J. Y. Chen, Y. N. Xia, *Nano Lett.* **2010**, *10*, 30–35.
- [16] a) J. Oliver-Meseguer, J. R. Cabrero-Antonino, I. Dominguez, A. Leyva-Perez, A. Corma, *Science* **2012**, *338*, 1452–1455; b) M. Shekhar, J. Wang, W. S. Lee, W. D. Williams, S. M. Kim, E. A. Stach, J. T. Miller, W. N. Delgass, F. H. Ribeiro, *J. Am. Chem. Soc.* **2012**, *134*, 4700–4708.
- [17] a) H. F. Duan, S. Sengupta, J. L. Petersen, N. G. Akhmedov, X. D. Shi, *J. Am. Chem. Soc.* **2009**, *131*, 12100–12102; b) K. Matyjaszewski, T. E. Patten, J. Xia, *J. Am. Chem. Soc.* **1997**, *119*, 674–680.
- [18] K. Matyjaszewski, J. H. Xia, *Chem. Rev.* **2001**, *101*, 2921–2990.
- [19] a) S. Barcikowski, G. Compagnini, *Phys. Chem. Chem. Phys.* **2013**, *15*, 3022–3026; b) C. J. Murphy, *Science* **2002**, *298*, 2139–2141.
- [20] a) A. K. Badu-Tawiah, C. P. Wu, R. G. Cooks, *Anal. Chem.* **2011**, *83*, 2648–2654; b) Z. Baird, W. P. Peng, R. G. Cooks, *Int. J. Mass Spectrom.* **2012**, *330*, 277–284.